Response to Reviewer #1's Comments:

Jiayi Li et al. (Author)

I am satisfied with the authors' responses and the revised manuscript. I have only a couple of remaining comments:

1. The authors state that warm invigoration at ECS occurs at high Nd, which contrasts with existing literature suggesting that collision–coalescence processes are typically delayed at low Nd. It would be helpful if the authors could elaborate further on this apparent discrepancy.

Response: Thanks for pointing this out! We acknowledge that the results in the ECS region are different from those in previous studies and attributing the positive LWP adjustments at high N_d solely to warm invigoration is insufficient. As suggested by the second reviewer's feedback, we performed a more detailed analysis of the increase in LWP at high N_d observed in the ECS region.

Our results indicate that this increase is likely attributed to the influence of cold air advection caused by prevailing northerly winds, especially for the period of spring and winter in the ECS region (Liu et al., 2016), which collectively account for ~75% of the samples. Coastal samples west of 125°E exhibit both high N_d and LWP under this continental flow (Fig. R1, A and G), because the advection of dry, cold, aerosol-rich air over warm SST enhances surface sensible and latent heat fluxes (Fig. R1, F, H, J and K) (Long et al., 2020), raising saturation vapor pressure and activating cloud droplets. This could be confirmed by a pronounced drop in $\Delta\theta_{950\text{-}surf}$ (potential temperature difference between 950 hPa and 2 m above the sea surface), revealing strong sub-cloud destabilization (Fig. R1I). This leads to an increase in saturated water vapor pressure then promoting the cloud droplet activation. Concurrently, high LTS along the coast (Fig. R1L) suppresses vertical mixing at cloud top (Scott et al., 2020), allowing activated droplets to accumulate more liquid water with thicker clouds (Fig. R1B) and higher CF (Fig. R1C). These meteorological co-variabilities jointly elevate N_d and LWP (and hence the N_d-LWP relationship) via cloud microphysical processes (Feingold et al., 2025).

The discussion about the increase in LWP at high N_d has been rephrased in the revised manuscript (see Lines 204-243): "In this study, the ascending branch of the V shape at high N_d condition (> ~300 cm^{-3}) is the main reason for the overall positive LWP adjustments in the ECS region. Positive sensitivity of LWP to N_d perturbations over the ECS has been reported but not fully understood (Bender et al., 2019; Gryspeerdt et al., 2019; Michibata et al., 2016; Zhang et al., 2021). Here, our results indicate a strong transition in meteorological conditions across the turning point of V shape (Fig. 2), suggesting large-scale meteorology as a possible driver.

Meteorological conditions significantly modulate cloud microphysical processes (e.g., cloud droplet activation, condensation, entrainment, collision-coalescence, and precipitation) (Feingold et al., 2025), which in turn alter both the sign and magnitude of LWP adjustments, particularly within the sharp environmental transition from coastal to offshore areas in the ECS region. Kuroshio Current produces a sharp SST gradient in the ECS region (shown in Fig. S4A), leading to a distinct transition in boundary layer thermodynamic structure and cloud properties from the coast to offshore areas (Liu et al., 2016). Following Rosenfeld et al. (2019), we categorize the clouds into three regimes, i.e., Sc (LTS > 18 K), Sc to Cu transition (14 K ≤ LTS ≤ 18 K), and Cu (LTS < 14 K) (Fig. S4, B, C, and D). Sc presents over a cooler sea surface along the coast (Fig. S4, A and B). The coastal distribution suggests that most of Sc may be advected from the Sc region in the southeast Chinese plain (Klein and Hartmann, 1993). According to the cloud advection scheme by Miller et al. (2018), cloud advection can be approximated as a translation of the cloud field with the wind field. The advection height is assumed to correspond to the height of the cloud top. Based on the 700 hPa wind field (Fig. S4A), it is plausible that Sc in the ECS region is possibly advected from the southeast Chinese plain. As air moves offshore, the cloud layer decouples with the surface mixed layer over the warmer sea surface—a process known as the "deepening-warming mechanism" (Albrecht et al., 1995). In this decoupled boundary layer, Cu forms in the moist and unstable subcloud layer and rises to the upper cloud layer, resulting in a locally cumulus-coupled MBL.

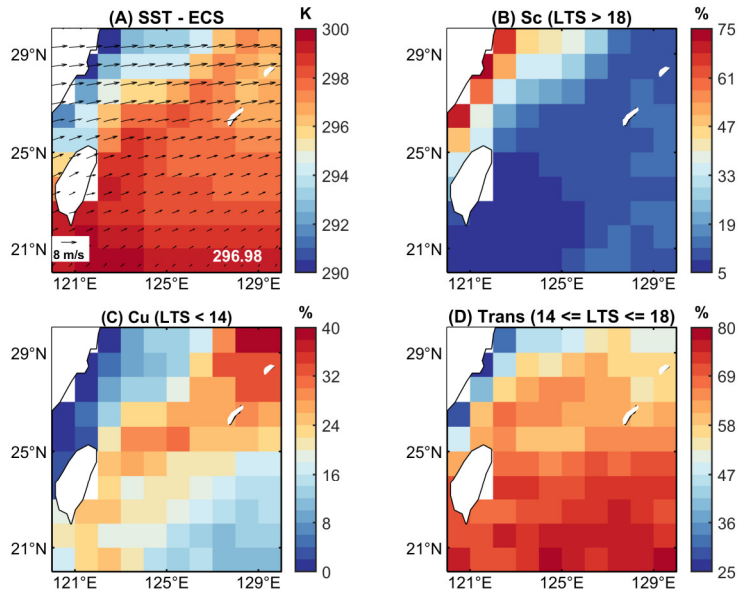

Figure S4. Distributions of meteorological factors and different cloud regimes in the ECS region. (A) Sea Surface Temperature (SST), the composite wind field (arrows) on 700 hPa. The numbers in the lower right corner represent regional averages being weighted by the cosine of latitude. Distributions of the proportion of cloud regimes for (B) Stratocumulus (Sc, LTS > 18 K), (C) Cumulus (Cu, LTS < 14 K), (D) Sc to Cu transition regime (Trans, 14 K <= LTS <= 18 K) are shown.

The cloud samples in the ascending branch are concentrated west of 125°E and dominated by continental air masses (Fig. 2A), which are characterized by strong northerly cold air advection at the surface that destabilizes the air-sea interface (Fig. 2, F and G). The potential temperature difference between 950 hPa and 2 m above the sea surface ($\Delta\theta_{950\text{-}surf}$) is calculated as an indicator of sub-cloud layer stability, revealing an extremely unstable sub-cloud layer in the ascending branch (Fig. 2I). Northerly winds transport relatively dry, cold, aerosol-rich air across the warm ocean (Fig. 2, F, G, and H). This destabilizes the sub-cloud layer and intensifies the upward fluxes of sensible and latent heat from sea surface into the atmosphere (Fig. 2, I, J and K) (Long et al., 2020), raising saturation water vapor pressure and facilitating cloud droplet activation. Additionally, high LTS along the coast (Fig. 2L) suppresses vertical mixing at cloud top (Scott et al., 2020), allowing activated droplets to accumulate more liquid water with thicker clouds (Fig. 2B) and higher CF (Fig. 2C). These conditions jointly elevate both N_d and LWP, forming the ascending branch of the V shape pattern.".

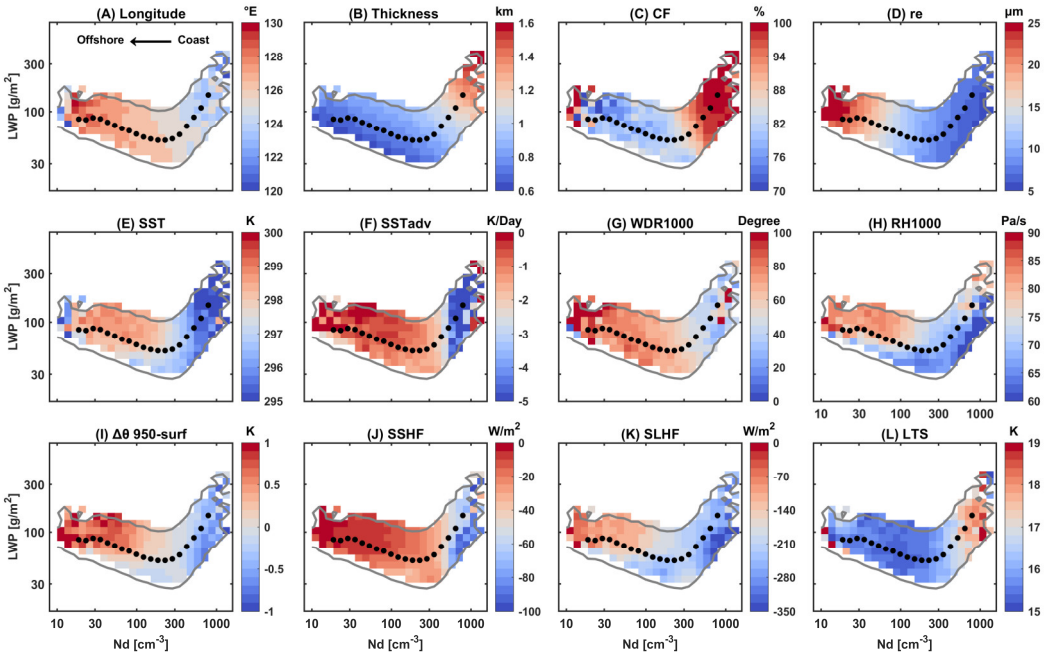

Figure R1. Distributions of meteorological conditions in N_d-LWP log-log space in the ECS region. The color scale represents the median values in each bin. Only bins with an occurrence of at least 5% are shown, bounded by the gray lines. (A) Longitude. (B) Cloud thickness. (C) Cloud fraction (CF). (D) Cloud effective radius (r_e). (E) Sea surface temperature (SST). (F) Horizontal temperature advection at the surface (SST_{adv}). (G) Wind direction on 1000 hPa. 0° indicates a northerly wind. (H) Relative humidity on 1000 hPa (RH1000). (I) The potential temperature difference between 950 hPa and 2 m above the sea surface ($\Delta\theta_{950\text{-}surf}$), a proxy of the sub-cloud layer stability. (J) Surface sensible heat flux (SSHF). (K) Surface latent heat flux (SLHF). For the vertical fluxes, the negative is upwards. (L) Lower-tropospheric stability (LTS). Black dots represent the median LWP in each N_d bins with a sample size greater than 50. **The figures are the same as Figure 2 in the revised manuscript.**

2. Line 497: Mesoscale organization has been shown to cause mesoscale variability in Nd (Zhou and Feingold, 2023), which partially explains the observed inconsistency between Nd and aerosol.

Zhou, X., & Feingold, G. (2023). Impacts of mesoscale cloud organization on aerosol- induced cloud water adjustment and cloud brightness. Geophysical Research Letters, 50(13), e2023GL103417

Response: We sincerely appreciate the reviewer's insightful reference to Zhou and Feingold (2023)and fully agree that mesoscale cloud organization can introduce variability in N_d independent of aerosol loading. As highlighted by Zhou and Feingold (2023), mesoscale cellular convections (MCCs) introduce spatial variability in N_d through scale-dependent processes. In small-scale MCCs, thicker cloud cores tend to have higher N_d due to more homogeneous depletion. In large-scale MCCs, the thicker cloud cores have lower N_d where precipitation scavenging dominates, while the non-precipitating cloud edges exhibit higher values.

We have added some discussions in the revised manuscript (see Lines 518-523): "Note that the correlations between AOD and N_d at certain fixed times are not statistically significant (not shown). This may be due to the relatively insignificant impact of aerosol effects at these moments, while other processes may exert a more pronounced influence. For example, strong boundary layer decoupling inhibits cloud droplet activations (Zeider et al., 2025). Mesoscale cloud organization can also introduce spatial heterogeneity in N_d independent of aerosol loading (Zhou and Feingold, 2023). Future research should broaden its scope to investigate the effects of other influencing factors on N_d at specific times, in addition to the role of aerosols.".

Reference

Albrecht, B. A., Bretherton, C. S., Johnson, D., Scubert, W. H., and Frisch, A. S.: The Atlantic Stratocumulus Transition Experiment—ASTEX, Bulletin of the American Meteorological Society, 76, 889–904, https://doi.org/10.1175/1520-0477(1995)076<0889:TASTE>2.0.CO;2, 1995.

Bender, F. A.-M., Frey, L., McCoy, D. T., Grosvenor, D. P., and Mohrmann, J. K.: Assessment of aerosol–cloud–radiation correlations in satellite observations, climate models and reanalysis, Clim Dyn, 52, 4371–4392, https://doi.org/10.1007/s00382-018-4384-z, 2019.

Feingold, G., Glassmeier, F., Zhang, J., and Hoffmann, F.: Opinion: Inferring Process from Snapshots of Cloud Systems, EGUsphere, 1–28, https://doi.org/10.5194/egusphere-2025-1869, 2025.

Gryspeerdt, E., Goren, T., Sourdeval, O., Quaas, J., Mülmenstädt, J., Dipu, S., Unglaub, C., Gettelman, A., and Christensen, M.: Constraining the aerosol influence on cloud liquid water path, Atmos. Chem. Phys., 19, 5331–5347, https://doi.org/10.5194/acp-19-5331-2019, 2019.

Liu, J.-W., Xie, S.-P., Yang, S., and Zhang, S.-P.: Low-Cloud Transitions across the Kuroshio Front

in the East China Sea, Journal of Climate, 29, 4429–4443, https://doi.org/10.1175/JCLI-D-15-0589.1, 2016.

Long, J., Wang, Y., Zhang, S., and Liu, J.: Transition of Low Clouds in the East China Sea and Kuroshio Region in Winter: A Regional Atmospheric Model Study, Journal of Geophysical Research: Atmospheres, 125, e2020JD032509, https://doi.org/10.1029/2020JD032509, 2020.

Michibata, T., Suzuki, K., Sato, Y., and Takemura, T.: The source of discrepancies in aerosol–cloud–precipitation interactions between GCM and A-Train retrievals, Atmos. Chem. Phys., 16, 15413–15424, https://doi.org/10.5194/acp-16-15413-2016, 2016.

Rosenfeld, D., Zhu, Y., Wang, M., Zheng, Y., Goren, T., and Yu, S.: Aerosol-driven droplet concentrations dominate coverage and water of oceanic low-level clouds, Science, 363, eaav0566, https://doi.org/10.1126/science.aav0566, 2019.

Scott, R. C., Myers, T. A., Norris, J. R., Zelinka, M. D., Klein, S. A., Sun, M., and Doelling, D. R.: Observed Sensitivity of Low-Cloud Radiative Effects to Meteorological Perturbations over the Global Oceans, Journal of Climate, 33, 7717–7734, https://doi.org/10.1175/JCLI-D-19-1028.1, 2020.

Zeider, K., McCauley, K., Dmitrovic, S., Siu, L. W., Choi, Y., Crosbie, E. C., DiGangi, J. P., Diskin, G. S., Kirschler, S., Nowak, J. B., Shook, M. A., Thornhill, K. L., Voigt, C., Winstead, E. L., Ziemba, L. D., Zuidema, P., and Sorooshian, A.: Sensitivity of aerosol and cloud properties to coupling strength of marine boundary layer clouds over the northwest Atlantic, Atmospheric Chemistry and Physics, 25, 2407–2422, https://doi.org/10.5194/acp-25-2407-2025, 2025.

Zhang, X., Wang, H., Che, H.-Z., Tan, S.-C., Yao, X.-P., Peng, Y., and Shi, G.-Y.: Radiative forcing of the aerosol-cloud interaction in seriously polluted East China and East China Sea, Atmospheric Research, 252, 105405, https://doi.org/10.1016/j.atmosres.2020.105405, 2021.

Zhou, X. and Feingold, G.: Impacts of Mesoscale Cloud Organization on Aerosol-Induced Cloud Water Adjustment and Cloud Brightness, Geophysical Research Letters, 50, e2023GL103417, https://doi.org/10.1029/2023GL103417, 2023.

Response to Reviewer #2's Comments:

Jiayi Li et al. (Author)

We highly appreciate the reviewer #2 for the valuable comments and constructive critiques, which have helped us improve the quality of our manuscript. Overall, we conducted further analysis of the V shape of LWP adjustments observed in the ECS region, including an investigation into the validity and potential causes of the results. Certain sections of the manuscript were reorganized to improve logical flow. Additionally, the language has been polished for clarity and readability.

In the following text, the reviewer's comments are listed in black, our response is in blue, and changes to the text are highlighted in red. A version of the revised manuscript with tracked changes is also provided.

1. The paper investigates the relationship between LWP and Nd for 2 regions over the Himawari domain. It is not clear why the authors select these regions, nor the motivation to carry out a regional analysis instead of investigating the full Himawari domain. Also, the English and the writing needs substantial work beyond the suggestions I provide here.

Response: We sincerely appreciate the reviewer's comment. The West Australia (AUW: 25°–35°S, 95°–105°E) and East China Sea (ECS: 20°–30°N, 120°–130°E) were selected due to their contrasting cloud regimes and environmental conditions. The AUW region represents relatively pristine subtropical Sc region and the ECS region represents polluted Sc-Cu transition clouds affected by high anthropogenic aerosols. These regions offer contrasting aerosol and meteorological regimes, allowing us to isolate and quantify how different environmental conditions modulate the N_d-LWP relationship.

The full Himawari domain encompasses a mixture of deep convection, frontal systems, and mid-/high-level clouds whose macro- and micro-physical properties differ markedly from warm Sc. Including such diverse cloud types would introduce high uncertainty of LWP and N_d retrievals (e.g., clouds with a thick optical thickness relative to stratocumulus clouds), large environmental heterogeneity, dilute the signal from the LWP adjustment mechanism we seek to investigate, and complicate the attribution of observed changes to aerosol versus meteorology. Nevertheless, even within the two chosen regions, the number of warm-cloud samples used in this study exceeds 10^5, ensuring robust statistics. Further studies with specific considerations as discussed above could be carried out for domain-wide data.

In the revised manuscript, we have clarified the scientific motivation for regional selection (see Lines 63-68): "Within the sight of Himawari-8, we selected two cloud regions with significantly different environmental backgrounds (see Fig. S1 in Supplementary Materials). One is a remote stratocumulus region located in the west of Australia (AUW: 25º-35ºS, 95º-105ºE) (Klein and Hartmann, 1993). The other is in the East China Sea (ECS: 20º-30ºN, 120º-130ºE), which is significantly impacted by anthropogenic aerosols and characterized by Sc to Cu transition (Long et al., 2020). The comparison between the two regions allows us to explore the regional differences of LWP adjustments and their potential driving mechanisms.

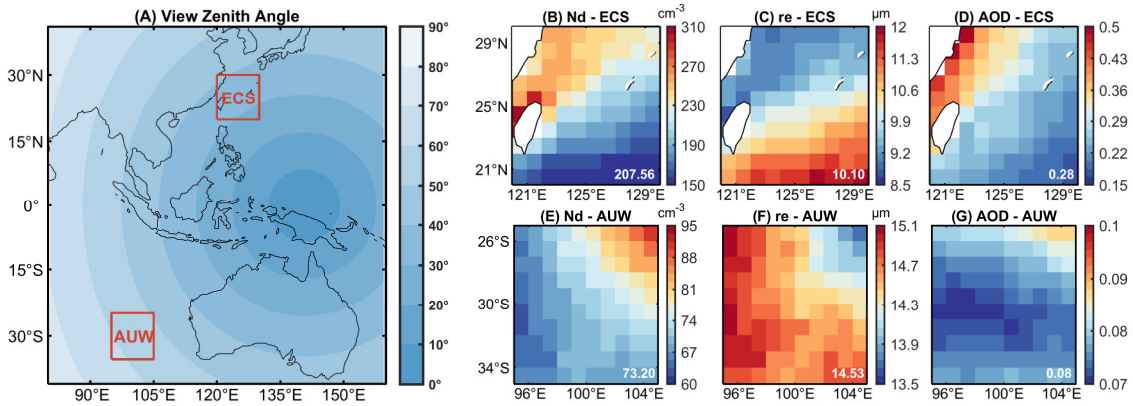

Figure S1. Distributions of cloud properties in two typical regions: the East China Sea (ECS: 20º-30ºN, 120º-130ºE) and the west of Australia (AUW: 25º-35ºS, 95º-105ºE). (A) Geographical distribution of the view zenith angle of Satellite Cloud and Radiation Property retrieval System (SatCORPS) Himawari-8 data. The selected regions are marked by red boxes. Spatial distributions of cloud droplet number concentration (N_d) (B, E), effective radius (r_e) (C, F) and total column aerosol optical depth (AOD) (D, G) from MERRA-2 data are presented. The numbers in the lower right corner represent regional averages being weighted by the cosine of latitude.".

We are also grateful for your feedback regarding the language and writing of our manuscript. We have carefully revised the manuscript to address these issues and ensure that the language is clear and accurate.

2. It is relevant to note that the precipitation filtering based on GPM observations will not remove light precipitation nor drizzle, which is quite persistent in these clouds. This is because GPM can detect rather large hydrometeors more typical of convective systems. In other words, this study is not limited to non-precipitating clouds, so precipitation must be considered when interpreting the results.

Response: Thanks for pointing this out! We agree with the reviewer that GPM cannot identify light precipitation nor drizzle. In fact, the presence of precipitation is recognized as a significant source of uncertainty in N_d retrievals (Grosvenor et al., 2018), thereby influencing the assessment of LWP adjustments. From the perspective of N_d retrieval accuracy, we thus filtered out precipitation events

to minimize the uncertainty. Although the majority of heavy precipitation has been screened out, a considerable amount of light precipitation remains that cannot be effectively detected by GPM. Here, we also have adopted a critical effective radius (r_e) threshold of 14 μm (Rosenfeld et al., 2012) to distinguish between drizzle-like clouds and non-drizzle clouds (see the black lines in Fig. R1), which is another widely used precipitation-identification method. The result does show a substantial proportion of precipitating samples remain in the dataset.

In the revised manuscript, we have explicitly recognized this limitation, and precipitation is therefore fully considered throughout our discussion and results. For example, the drizzle-like samples in both regions exhibit a weaker negative LWP adjustment, which may be attributed to precipitation suppression driven by increased N_d that weakens the entrainment-feedbacks (Fig. R1).

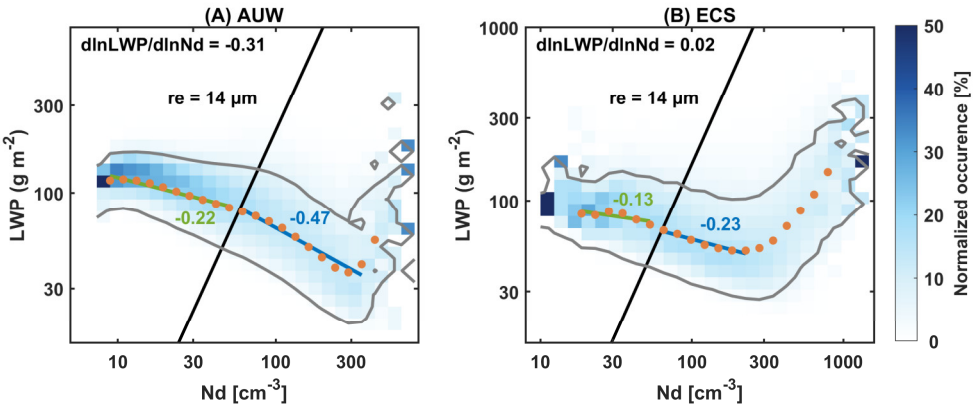

Figure R1. Joint histograms of N_d and LWP in log-log space in the AUW and ECS regions. The column of each N_d bin is normalized. The black lines are fitted based on the bins in the joint histogram with the effective radius (r_e) closest to 14 μm. The gray lines represent the contour of 5% occurrence. Orange dots represent the median LWP in each N_d bins with a sample size greater than 50. The green and blue lines are regression slopes for the orange points with r_e above and below 14 μm, respectively. **The figures are the same as Figure 1 in the revised manuscript.**

As suggested, the discussion of the precipitation filtering has been rephrased on Lines 126-131: "To minimize the influence of precipitation on N_d and LWP retrievals, GPM IMERG Final Precipitation L3 Half Hourly 0.1 degree x 0.1 degree V07 (GPM_3IMERGHH) was used (Huffman et al., 2020). Cloud samples were included in the analysis only if the GPM_3IMERGHH precipitation rate equals 0 mm/hr in a 1° × 1° grid. To align these two satellite products, SatCORPS cloud pixels within each 0.1° grid of GPM_3IMERGHH are assigned the same precipitation value. Considering the limited ability of GPM to detect light precipitation and drizzle, we additionally applied a r_e = 14 μm threshold to distinguish between drizzle scenes and non-drizzle scenes (black lines in Fig. 1).".

In addition, we have expanded the discussion to more explicitly address the influence of precipitation on our findings on Lines 192-196: "For instance, samples with r_e > 14 μm—conditions more likely to contain drizzle (Rosenfeld et al., 2012)—still exhibit a weaker negative LWP

adjustment than those with r_e < 14 μm (Fig. 1, –0.22 vs. –0.47 in the AUW and -0.13 vs. -0.23 in the ECS), consistent with the results of Zhou and Feingold (2023) in the northwestern Atlantic. It suggests that in drizzle-like samples, the precipitation suppression partially offsets the dominant LWP reduction caused by the entrainment effect, resulting in a weak decrease in LWP with increasing N_d compared to non-drizzle samples.".

3. The most interesting result of this study is the positive correlation between LWP and Nd for high values of Nd. The authors conducted a partial assessment of the relationship, but it is still a somewhat superficial analysis. A critical question is whether the finding is physical. To that end, it is recommended to analyze variability of Nd and LWP with cloud fraction because biases in broken scenes could well explain the relationship. Also the result might be dependent on the binning methods. Is the binning based on percentiles, that is, bins with the same number of samples?

Response: We appreciate the reviewer's insightful comments. As suggested, we have confirmed the robustness of the positive N_d-LWP relationship at high N_d through further analysis.

(1) **Influence of broken scenes:** The impact of broken scenes on our results is extremely limited. Figure R2 presents the distribution of CF in N_d-LWP space and the sensitivity analysis of the results to different CF groups. The increase in LWP at high N_d aligns with an increase in CF (Fig. R2A). Following Cao et al. (2023), a CF of 80% was used to distinguish between cloudy and broken scenes. For both cloudy scenes (CF > 80%) and broken scenes (CF < 80%), the increase in LWP at high N_d consistently exists (Fig. R2, B and C). In addition, the average CF for samples of positive correlation between LWP and N_d (> ~300 cm^{-3}) is 86% (not the broken scenes). Therefore, the observed increase in LWP at high N_d cannot be attributed to broken scenes.

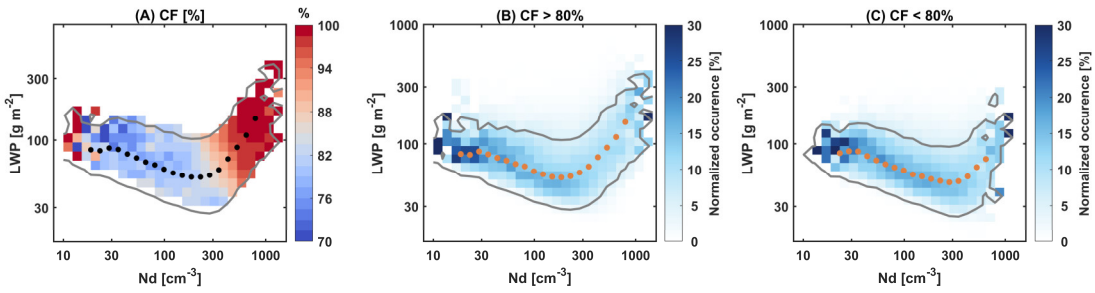

Figure R2. (A) The median cloud fraction (CF) in N_d-LWP log-log space in the ECS region. Only the bins with at least 5% occurrence are shown, bounded by the gray line. Panels (B) and (C) show the normalized joint histograms of N_d and LWP in log-log space in the ECS region, with CF greater than 80% and less than 80%, respectively. Black and orange dots represent the median LWP in each N_d bins with a sample size greater than 50. **The figures are same as Figure S3 in the revised Supplementary Materials.**

(2) **Influence of binning methods.** This study employs equal-width binning based on equal log(N_d)

intervals. To minimize the noise of sparse samples, only the N_d bins containing more than 50 samples were used to calculate the LWP adjustment. The main reason for choosing equal-width binning was to preserve the original physical scale of the samples, avoiding the excessive smoothing of samples with diverse meteorological conditions gathered in a single bin using equal-sample binning (Towers, 2014). Figure R3 compares results using two binning methods, both consistently showing an LWP increase at high N_d. Thus, the positive N_d-LWP correlation at high N_d is not artificially induced by the binning methodology.

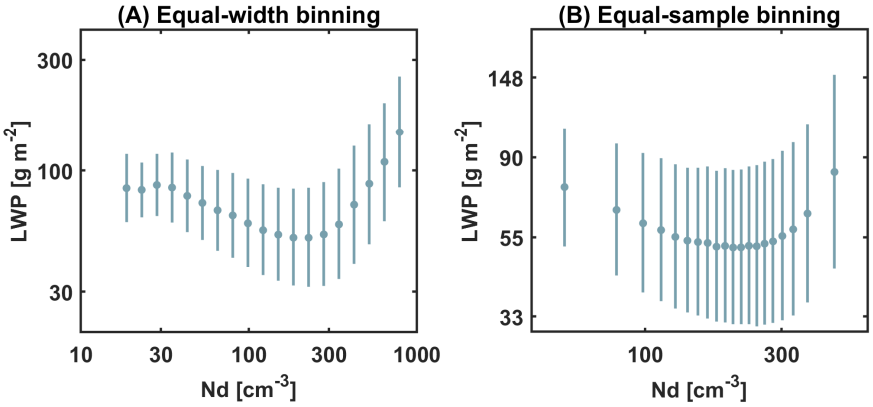

Figure R3. Comparison of the N_d-LWP relationship using two binning methods.

Based on the above results, we have added detailed discussions on the impact of the broken scenes and the binning method in the revised manuscript:

Lines 178-182: "To investigate whether the positive N_d-LWP relationship is influenced by broken scenes, we assessed the sensitivity of our results to CF. As shown in Fig. S3, the rise in LWP at high N_d coincides with an increase in CF. The average CF for samples with N_d > 300 cm^{-3} is 86%. Additionally, the positive N_d-LWP relationship persists in both overcast (CF > 80%) and broken (CF < 80%) cloud scenes. This consistency indicates that the observed LWP increase at high N_d is unlikely to be an artifact of broken-cloud scenes.".

Lines 141-147: "LWP adjustment at any given moment is the result of all available data at that moment. The regression slope of N_d and LWP in log-log space ($\frac{\partial \ln LWP}{\partial \ln N_d}$) is calculated on 1° grid scale. We employed equal-width binning, using the median LWP within each N_d bin to regress the slope. To reduce noise from sparse samples, only bins with more than 50 samples were used to calculate LWP adjustments. Additionally, we tested the equal-sample binning method. The patterns of the N_d-LWP relationship and diurnal variations of LWP adjustments remained robust across different binning methods. The main reason for choosing equal-width binning was to preserve the original physical scale of the samples, avoiding the excessive smoothing of samples with diverse meteorological conditions gathered in a single bin using equal-sample binning (Towers, 2014).".

For a detailed explanation of the positive correlation between LWP and N_d at high N_d, please refer to the response to Comment 18.

4. Abstract, "Their reflectivity to solar radiation is highly sensitive to atmospheric aerosol concentrations because aerosols can serve as the cloud condensation nuclei (CCN) to modify the mediated variables (e.g. droplet number concentrations, Nd; effective radius, re) of aerosol-cloud interactions (ACI)". The sentence does not make sense grammatically.

…while holding cloud liquid water content (the Twomey effect) (Twomey, 1977). What does it mean?

Response: Thank you for your careful review. We acknowledge that the original sentences were not expressed clearly and have rephrased the sentences accordingly (see Lines 24-29): "Cloud reflectivity to solar radiation is highly sensitive to atmospheric aerosol concentrations. Because aerosols can serve as the cloud condensation nuclei (CCN), which modify key microphysical variables such as cloud droplet number concentrations (N_d) and droplet effective radius (r_e). For a given cloud liquid water content, aerosol-induced increases in CCN can enhance N_d and hence reduce r_e, boosting cloud albedo (Twomey, 1977), which is known as cloud albedo effect, being an important component of aerosol-cloud interactions (ACI).".

5. Line 60, it should be "non-precipitating"

Response: Thank you for your careful review. The mistake has been corrected.

6. Line 83: "Nd can be estimated"….be more specific, did you use Eq. (1)?, If the answer is YES, then say it: "Nd IS estimated"

Response: Thanks for your comment! We confirm that N_d was calculated by Eq. (1). We have revised the sentence as the reviewer suggested.

7. Line 77: "Briefly, CLTH is estimated as the altitude where the cloud-top temperature (CLTT) occurs in the temperature profile." This assertion is incorrect, SatCORPS does not directly use the profile and the retrieved temperature for deriving the cloud height. Instead, the method is based on a lapse rate approach. See Sun-Mack et al., 2014:

Sun-Mack, S., P. Minnis, Y. Chen, S. Kato, Y. Yi, S. C. Gibson, P. W. Heck, and D. M. Winker, 2014: Regional Apparent Boundary Layer Lapse Rates Determined from CALIPSO and MODIS Data for Cloud-Height Determination. J. Appl. Meteor. Climatol., 53, 990–1011, https://doi.org/10.1175/JAMC-D-13-081.1.

Response: We appreciate the reviewer's comment and apologize for the incorrect descriptions. We

have revised the sentence (see Lines 84-86): "Briefly, for boundary layer clouds, CLTH is retrieved using a lapse rate method: $\Gamma_b = (CET - T_0)/(\mathrm{CLTH} - Z_0)$ (Sun-Mack et al., 2014). Cloud effective temperature (CET) was estimated from the Infrared Window (IRW) channel. Z_0 denotes the surface elevation and T_0 is the sea surface temperature.".

8. Line 74: "retrieve Nd" do you mean "calculate Nd"?

Response: Thanks for your comment! We have replaced 'retrieve' with 'calculate' to ensure an accurate description.

9. Line 76-77 The SatCORPS is based on the CERES Ed4 cloud retrieval algorithm, providing more accurate CLTH and H parameterizations (Minnis et al., 2011, 2021)." More accurate than what?

Response: Thanks for your comment! We have clarified the sentence in the revised manuscript(see Lines 82-83): "The SatCORPS product is based on the CERES Ed4 cloud retrieval algorithm (Minnis et al., 2021), which provides more accurate parameterizations of CLTH and H than the CERES Edition 2 retrieval algorithm (Minnis et al., 2011).".

10. Line 79: "CLTT is derived from an empirical parameterization of cloud-top emissivity at channel 4 and cloud effective temperature." This correction primarily applies to thin cirrus clouds. For boundary layer clouds, effective and cloud top temperature are identical. Remove the sentence.

Response: We are grateful for your comment! We have removed the sentence as suggested.

11. Line 82: "The SatCORPS retrievals provide cloud effective radius (re) in the 3.9 μm near-infrared band". Please, be accurate with your description. It is more clear to say: "SatCORPS cloud droplet effective radius (re) is primarily estimated from the 3.9um near-infrared band"

Response: We sincerely apologize for the inaccurate description. We have revised the sentence as suggested.

12. Line 86: "as Q relies less on the size parameter in near-infrared." The sentence does not make sense. Do you mean that Q varies little with particle size?

Response: Thank you for raising this question. We acknowledge that the description here is inaccurate. Q is the extinction efficiency factor. The size parameter is the ratio of the particle size to the wavelength ($\chi = \frac{2\pi r}{\lambda}$)is the particle size ($r$) and wavelength ($\lambda$). For liquid cloud droplets (~10 μm), the geometric optics limit is almost reached because $r \gg \lambda$ in the visible wavelength range (0.65–0.86 μm), and thus Q is approximately equal to its asymptotic value of 2 (Grosvenor et al., 2018). We have rephrased the sentence to be clear in the revised manuscript (see Line 92): "The extinction efficiency factor $Q \approx 2$.".

13. Lines 106: “We followed the previous methods to filter cloud pixels. But this classification…”, Why classification? Please revise the sentence.

Response: Thank you for your comment. We have rephrased the sentence to be clearer (see Lines 111-112): “We followed the above methods to filter cloud pixels, which only limit cloud top properties and cloud phase, inevitably including different cloud regimes, such as low-level cumulus clouds.”.

14. Line 106-108, Why do you say that departures from adiabaticity are different between cumulus and stratocumulus clouds? This is a speculative statement.

Response: Thank you for pointing this out. We agree that this is a speculative statement. However, it is grounded in multiple lines of published evidence rather than pure conjecture. Below shows the reasons.

Cumulus clouds are subject to stronger lateral entrainment driven by their larger vertical velocity shear and smaller aspect ratio (Heus et al., 2008). Stratocumulus, capped by strong inversions and often driven by cloud-top radiative cooling, entrains primarily at the top (Mellado, 2017); this ventilation affects the upper portion but leaves the lower portion closer to adiabatic. The difference in entrainment processes significantly impacts their adiabatic profiles. Small et al. (2013) found that the adiabatic fraction (f_{ad}, defined as the ratio of actual LWC to adiabatic LWC) of cumulus clouds showed no significant variation with height. However, Wood (2005) observed that the adiabaticity in stratocumulus clouds decreased from cloud base to cloud top.

Vertical soundings and aircraft penetrations repeatedly show that shallow continental cumuli often exhibit strong dilution and large negative buoyancy within a few hundred meters above cloud base (e.g. Drueke et al., 2020). In contrast, stratocumulus layers sampled during DYCOMS-II, VOCALS-REx and SOCRATES retain near-adiabatic cores over the upper 30-50% of the cloud layer (Stevens et al., 2003; Wang et al., 2021; Wood et al., 2011). The difference is quantified by the f_{ad}, whose median values are 0.25-0.40 for cumulus and 0.7-0.9 for stratocumulus. Except for in-situ aircraft data, satellite observations (e.g., MODIS/CloudSat) collocations show that the slope of LWP versus cloud depth is markedly lower in cumulus scenes than in stratocumulus (Michibata et al., 2021), implying larger departures from the adiabatic LWP profile.

Therefore, to ensure the accuracy of this statement, we have added the relevant references to support this speculative statement in the revised version (see Line 112-118): “This might introduce uncertainties as cumulus clouds and stratocumulus clouds have different adiabatic properties, but we have set f_{ad} as a constant value in N_d calculations. Small et al. (2013) found that the f_{ad} of cumulus clouds showed no significant variation with height, whereas Wood (2005) observed that the

adiabaticity in stratocumulus clouds decreased from cloud base to cloud top. The difference in departures from adiabaticity between cumulus and stratocumulus stems from their different entrainment processes. Stratocumulus clouds are primarily influenced by the entrainment of dry air at cloud top (Mellado, 2017). In contrast, cumulus clouds are dominated by lateral entrainment (Heus et al., 2008).".

15. Line 115: "Consequently, the above uncertainties will not greatly affect the conclusions of this paper…" We do not really know. For instance, if retrievals uncertainties are a function of solar zenith angle, then uncertainties will change with local time… Also, hourly changes in entrainment rate can modify the Fad parameter.

Response: Thank you for your careful reading. We acknowledge that the above phrasing is not precise. To date, there is no robust method to improve the uncertainties discussed in our paper (namely, the impact of constant f_{ad} and k values). Consequently, f_{ad} and k are generally assumed to be constant in almost all studies investigating the diurnal variation of LWP adjustments based on geostationary satellite (Fons et al., 2023; Qiu et al., 2024; Smalley et al., 2024). This simplification is not arbitrary: in-cloud aircraft data show that k is nearly invariant above the lower half of warm clouds (Brenguier et al., 2011; Martin et al., 1994), and satellite-based f_{ad} climatology indicates standard deviations < 15% for extensive stratocumulus decks (Painemal and Zuidema, 2011). Nevertheless, k and f_{ad} do exhibit systematic vertical and cloud-type dependencies, and ignoring these variations can bias retrieved N_d by up to 30 % (Grosvenor et al., 2018). In the absence of global, high-resolution k and f_{ad} products, however, constant values remain the best practical compromise. Dedicated airborne campaigns that simultaneously measure cloud microphysics, vertical structure, and radiation are therefore essential to reduce these residual uncertainties for future studies.

We have revised the relevant descriptions (see Lines 119-125): "As acquiring hourly f_{ad} on a global scale is rather difficult, to date, studies investigating diurnal variations of LWP adjustments based on geostationary satellites continue to employ a constant f_{ad} value (Fons et al., 2023; Qiu et al., 2024; Smalley et al., 2024). Also, the choices of a constant k might introduce bias into the retrieval of N_d (Grosvenor et al., 2018). Studies have found that k parameter varied with the height within cloud and cloud types (Brenguier et al., 2011; Martin et al., 1994; Painemal and Zuidema, 2011). This indicates that the presence of diurnal variations in k and f_{ad} (e.g., hourly changes in entrainment rate can modify f_{ad}) introduces further bias. The resulting uncertainties warrant further in situ observation to improve the accuracy.".

16. Line 125: I disagree. I direct way to calculate the effects of aerosols on LWP is to actually use aerosol concentration rather Nd. True, we don't have aerosol retrievals for doing these….Please,

change the "direct way" sentence….perhaps you could say: "is the standard way to quantify LWP sensitivity to aerosol from satellite data".

Response: Thank you for your comment! We have revised the sentences as suggested (see Lines 133-136): "The logarithmic relationship between N_d and LWP ($\frac{\partial \ln LWP}{\partial \ln N_d}$) is the standard way to quantify LWP sensitivity to aerosol from satellite data, where N_d is considered a proxy of CCN. Another way of describing the changes of cloud water due to aerosols ($-\frac{\Delta \ln \tau}{\Delta \ln r_e}$) is deduced from the contributions of changes in LWP and r_e to the changes in cloud optical depth ($\frac{\Delta \tau}{\tau} = \frac{\Delta LWP}{LWP} - \frac{\Delta r_e}{r_e}$).".

17. Line 144: "obtained or calculated by ERA5 reanalysis"….What does it mean? Just say that the atmospheric parameters are obtained from ERA5.

Response: Thanks for your suggestion. We have rephrased the sentence as suggested.

18. Line 176. "For non-precipitation clouds, both positive and negative LWP adjustments have been reported" This is correct but all these studies report an inverted-V shape, whereas this study show a V shape. This is a substantial difference, which needs to be further explored. Finding a V-shape is significant departure from previous studies and, thus, the authors should spend more time trying to understand these results and double test check the signature is real.

Response: We thank the reviewer for raising valuable suggestions and great questions! We conducted a more comprehensive assessment of the V-shape and attribute the difference between our results and the established inverted-V pattern primarily to two factors:

(1) **Limited pristine conditions in our study regions.** The inverted-V shape is associated with positive LWP adjustments at low N_d, which have been linked to precipitation suppression (Albrecht, 1989; Glassmiere et al., 2021). That is, as increasing N_d, the reduced r_e may enhance the stability against coalescence and suppress the precipitation and loss of LWP (Albrecht, 1989; Glassmeier et al., 2021). The positive slopes at low N_d are typically observed in very pristine conditions especially when N_d is below approximately 10 cm^{-3} (Fons et al., 2023; Goren et al., 2025). However, in this study, 98% of the AUW samples have N_d above 15 cm^{-3}, and 99% of the ECS samples have N_d above 30 cm^{-3}. This explains the absence of a significant positive slope at low N_d. However, this LWP increase resulting from precipitation suppression is still detectable in our study. In drizzle-like clouds (r_e > 14 μm), we observe a less negative slope than in non-drizzle clouds (Fig. R1, -0.22 vs. -0.47 in the AUW and -0.13 vs. -0.23 in the ECS), which aligns with results of Zhou and Feingold (2023) in the Northwest Atlantic. It suggests that in drizzle-like samples, the precipitation suppression partially offsets the dominant LWP

reduction caused by entrainment effect, resulting in a weak decrease in LWP with increasing N_d compared to non-drizzle samples.

(2) Strong transition of meteorological conditions across the turning point of V-shape. Figure R4 shows the distribution of meteorological conditions in N_d-LWP log-log space. In the ECS region, where the V-shape is prominent, the samples exhibit strong geographic dependence. Coastal samples west of 125°E exhibit both high N_d and LWP under northerly continental flow (Fig. R4, A and G),especially for the period of spring and winter in the ECS region (Liu et al., 2016), which accounts for 75% of the samples. Northerly advection of dry, cold, aerosol-rich air contrasts sharply with the warm ocean surface and enhances surface heat fluxes (SSHF) and surface latent fluxes (SLHF) from ocean to the atmosphere (Fig. R4, F, H, J and K) (Long et al., 2020), raising saturation vapor pressure and activating cloud droplets. This could be confirmed by a pronounced drop in $\Delta\theta_{950\text{-surf}}$ (potential temperature difference between 950 hPa and 2 m above the sea surface), revealing strong sub-cloud destabilization (Fig. R4I). Additionally, high LTS along the coast (Fig. R4L) suppresses vertical mixing at cloud top (Scott et al., 2020), allowing activated droplets to accumulate more liquid water with thicker clouds (Fig. R4B) and higher CF (Fig. R4C). These meteorological co-variabilities jointly elevate N_d and LWP (and hence N_d-LWP relationship) via cloud microphysical processes (Feingold et al., 2025).

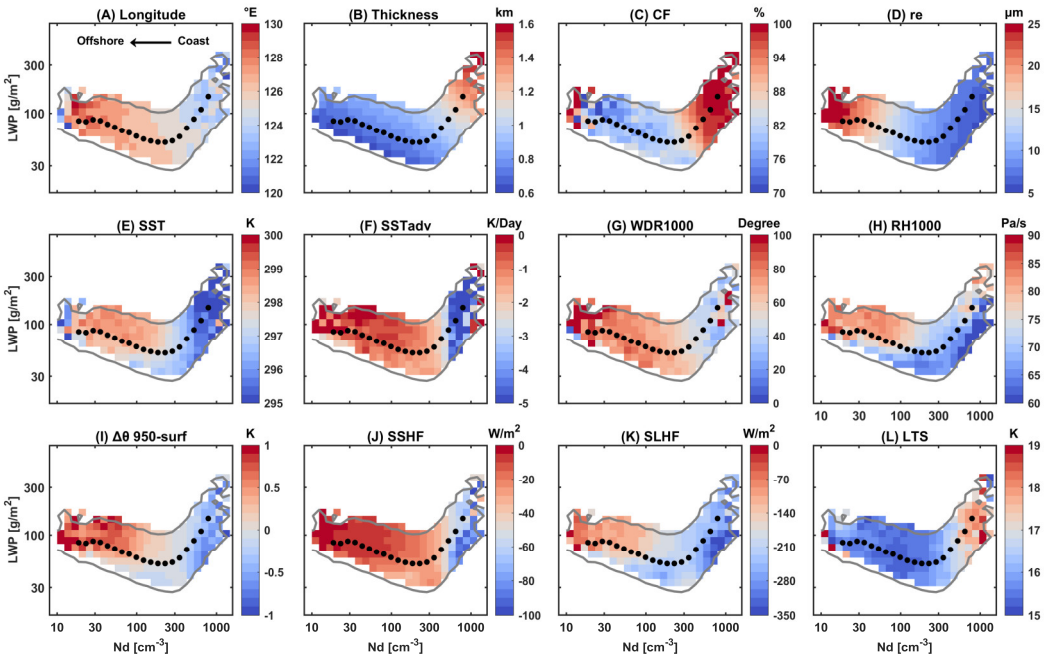

Figure R4. Distributions of meteorological conditions in N_d-LWP log-log space in the ECS region. The color scale represents the median values in each bin. Only bins with an occurrence of at least 5% are shown, bounded by the gray lines. (A) Longitude. (B) Cloud thickness. (C) Cloud fraction (CF). (D) Cloud effective radius (r_e). (E) Sea

surface temperature (SST). (F) Horizontal temperature advection at the surface (SST_{adv}). (G) Wind direction on 1000 hPa. 0° indicates a northerly wind. (H) Relative humidity on 1000 hPa (RH1000). (I) The potential temperature difference between 950 hPa and 2 m above the sea surface ($\Delta\theta_{950\text{-}surf}$), a proxy of the sub-cloud layer stability. (J) Surface sensible heat flux (SSHF). (K) Surface latent heat flux (SLHF). For the vertical fluxes, the negative is upwards. (L) Lower-tropospheric stability (LTS). Black dots represent the median LWP in each N_d bins with a sample size greater than 50. **The figures are the same as Figure 2 in the revised manuscript.**

In the revised manuscript, we have added a more detailed discussion on the V shape (see Lines 183-243): "The V shape observed in our results differs from the inverted-V shape reported in previous studies (Glassmeier et al., 2021; Gryspeerdt et al., 2019). Specifically, it is characterized by the absence of an ascending branch at low N_d and the emergence of an ascending branch at high N_d. The inverted-V shape is typically associated with positive LWP adjustments at low N_d, which have been linked to precipitation suppression (Albrecht et al., 1995). That is, as increasing N_d, the reduced r_e may enhance the stability against coalescence and suppress the precipitation and loss of LWP (Albrecht, 1989; Glassmeier et al., 2021). The positive slopes are often observed in very pristine environments (Gryspeerdt et al., 2023), especially when N_d is below approximately 10 cm^{-3} (Fons et al., 2023; Goren et al., 2025). In contrast, in this study, 98% of the AUW samples exhibit N_d values exceeding 15 cm^{-3}, and 99% of the ECS samples have N_d greater than 30 cm^{-3}. Therefore, we did not find this positive slope of the inverted-V shape. Nevertheless, the LWP increasing signal resulting from precipitation suppression is still detectable in our study. For instance, samples with r_e > 14 μm—conditions more likely to contain drizzle (Rosenfeld et al., 2012)—still exhibit a weaker negative LWP adjustment than those with r_e < 14 μm (Fig. 1, –0.22 vs. –0.47 in the AUW and -0.13 vs. -0.23 in the ECS), consistent with the results of Zhou and Feingold (2023) in the northwestern Atlantic. It suggests that in drizzle-like samples, the precipitation suppression partially offsets the dominant LWP reduction caused by the entrainment effect, resulting in a weak decrease in LWP with increasing N_d compared to non-drizzle samples.

In this study, the ascending branch of the V shape at high N_d condition (> ~300 cm^{-3}) is the main reason for the overall positive LWP adjustments in the ECS region. Positive sensitivity of LWP to N_d perturbations over the ECS has been reported but not fully understood (Bender et al., 2019; Gryspeerdt et al., 2019; Michibata et al., 2016; Zhang et al., 2021). Here, our results indicate a strong transition in meteorological conditions across the turning point of V shape (Fig. 2), suggesting large-scale meteorology as a possible driver.

Meteorological conditions significantly modulate cloud microphysical processes (e.g., cloud droplet activation, condensation, entrainment, collision-coalescence, and precipitation) (Feingold et al., 2025), which in turn alter both the sign and magnitude of LWP adjustments, particularly within the sharp environmental transition from coastal to offshore areas in the ECS region. Kuroshio Current

produces a sharp SST gradient in the ECS region (shown in Fig. S4A), leading to a distinct transition in boundary layer thermodynamic structure and cloud properties from the coast to offshore areas (Liu et al., 2016). Following Rosenfeld et al. (2019), we categorize the clouds into three regimes, i.e., Sc (LTS > 18 K), Sc to Cu transition (14 K ≤ LTS ≤ 18 K), and Cu (LTS < 14 K) (Fig. S4, B, C, and D). Sc presents over a cooler sea surface along the coast (Fig. S4, A and B). The coastal distribution suggests that most of Sc may be advected from the Sc region in the southeast Chinese plain (Klein and Hartmann, 1993). According to the cloud advection scheme by Miller et al. (2018), cloud advection can be approximated as a translation of the cloud field with the wind field. The advection height is assumed to correspond to the height of the cloud top. Based on the 700 hPa wind field (Fig. S4A), it is plausible that Sc in the ECS region is possibly advected from the southeast Chinese plain. As air moves offshore, the cloud layer decouples with the surface mixed layer over the warmer sea surface—a process known as the "deepening-warming mechanism" (Albrecht et al., 1995). In this decoupled boundary layer, Cu forms in the moist and unstable subcloud layer and rises to the upper cloud layer, resulting in a locally cumulus-coupled MBL.

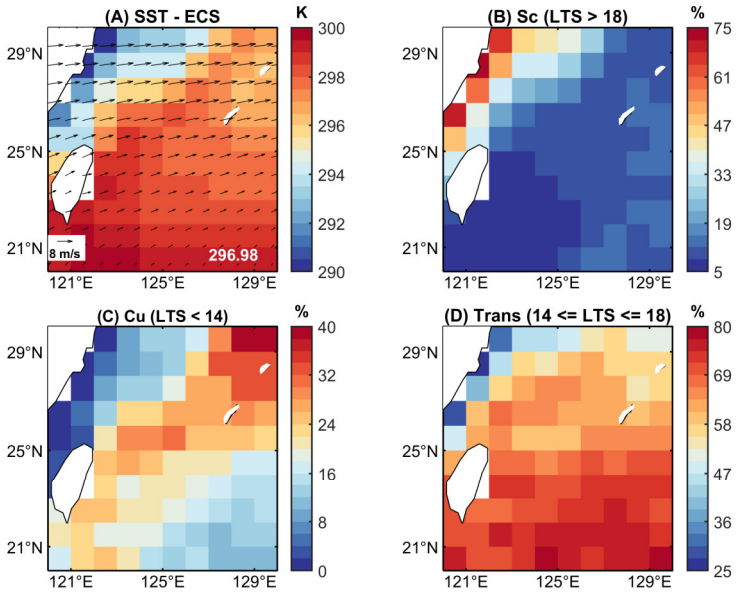

Figure S4. Distributions of meteorological factors and different cloud regimes in the ECS region. (A) Sea Surface Temperature (SST), the composite wind field (arrows) on 700 hPa. The numbers in the lower right corner represent regional averages being weighted by the cosine of latitude. Distributions of the proportion of cloud regimes for (B) Stratocumulus (Sc, LTS > 18 K), (C) Cumulus (Cu, LTS < 14 K), (D) Sc to Cu transition regime (Trans, 14 K <= LTS <= 18 K) are shown.

The cloud samples in the ascending branch are concentrated west of 125°E and dominated by continental air masses (Fig. 2A), which are characterized by strong northerly cold air advection at the surface that destabilizes the air-sea interface (Fig. 2, F and G). The potential temperature difference between 950 hPa and 2 m above the sea surface ($\Delta\theta_{950\text{-}surf}$) is calculated as an indicator

of sub-cloud layer stability, revealing an extremely unstable sub-cloud layer in the ascending branch (Fig. 2I). Northerly winds transport relatively dry, cold, aerosol-rich air across the warm ocean (Fig. 2, F, G, and H). This destabilizes the sub-cloud layer and intensifies the upward fluxes of sensible and latent heat from sea surface into the atmosphere (Fig. 2, I, J and K) (Long et al., 2020), raising saturation water vapor pressure and facilitating cloud droplet activation. Additionally, high LTS along the coast (Fig. 2L) suppresses vertical mixing at cloud top (Scott et al., 2020), allowing activated droplets to accumulate more liquid water with thicker clouds (Fig. 2B) and higher CF (Fig. 2C). These conditions jointly elevate both N_d and LWP, forming the ascending branch of the V shape pattern.".

19. Line 344 why is unexpected that the AOD diurnal cycle is flat? This is absolutely expected, especially over oceanic regions. Variations in AOD should be minimal, especially away from the aerosol sources.

Response: We agree with the reviewer's comment. We have removed the inappropriate description and revised the sentences (see Line 357-360): "N_d continually declines from 0700 LT to 1600 LT and r_e does not change significantly before 1200 LT and then rises. In contrast, there is no evident diurnal variation of AOD in the AUW, which is reasonable in the remote ocean area but insufficient to explain the diurnal variations of N_d and r_e. This suggests that other factors rather than aerosols may be responsible for the diurnal variations of N_d and r_e over the AUW region.".

20. Line 437. The reference should be Painemal et al. 2017.

Response: Thanks for raising this question. We have corrected the reference.

21. Section 3.3. Without considering diurnal variations in Nd and albedo, the whole sensitivity calculation has no validity.

Response: We agree with the reviewer's point and acknowledge our oversight in the manuscript. To address this issue, we calculated cloud albedo (A_c) from cloud optical depth (τ) based on a general expression for the two-stream approximation solution (Glenn et al., 2020):

$$A_c = \frac{\tau}{13.33 + \tau} \quad (1)$$

The susceptibility of A_c to N_d (S) is estimated as (Bellouin et al. 2020):

$$S = \frac{dA_C}{d\,ln\,N_d} = \frac{A_C(1 - A_C)}{3}\left(1 + \frac{5}{2}\frac{d\,ln\,LWP}{d\,ln\,N_d}\right) \quad (2)$$

Based on the above formula, we calculated S using MODIS-averaged value (Terra at 1030 LT and Aqua at 1330 LT) for either A_c or LWP adjustments while retaining the diurnal variation for the

other (Fig. R5). Given the minimal diurnal fluctuation in $\frac{A_C(1-A_C)}{3}$, the diurnal variations of S are mainly controlled by LWP adjustments. Therefore, considering the diurnal variability of A_c would not significantly affect our results.

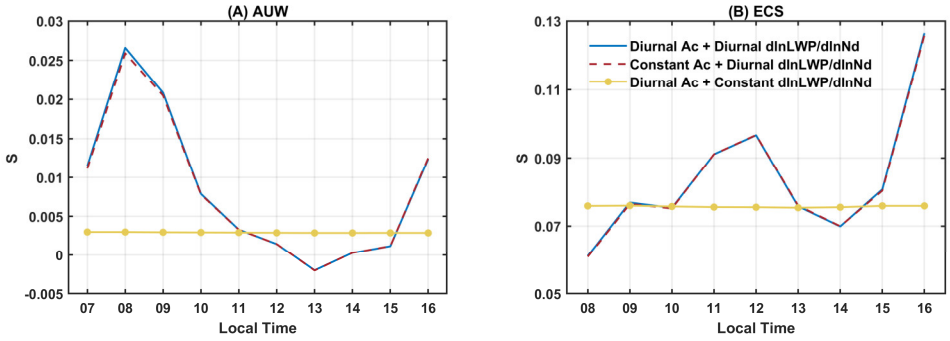

Figure R5. The susceptibility (S) of A_c to N_d calculated by Eq. (2) under three input combinations in the (A) AUW and (B) ECS regions: (1) diurnally varying A_c and dlnLWP/dlnN_d, (2) MODIS-averaged A_c (Terra at 1030 LT and Aqua at 1330 LT) and diurnally varying dlnLWP/dlnN_d, and (3) MODIS-averaged dlnLWP/dlnN_d and diurnally varying A_c. **The figures are the same as Figure S18 in the revised Supplementary Materials.**

In the revised manuscript, Section 3.3 has been rephrased and incorporated into Discussion section for better flow (see Lines 464-486):

"As discussed above, regional geostationary observations reveal the significant impact of regional diurnal dynamic processes on LWP adjustments, ranging from –0.41 to –0.27 in the AUW and from –0.11 to 0.21 in the ECS. Assuming a constant LWP adjustment based on polar-orbiting snapshots, rather than considering its diurnal variations will ultimately affect the estimation of the aerosol indirect effect. The cloud albedo (A_c) susceptibility to aerosols perturbations is estimated as (Bellouin et al. 2020):

$$S = \frac{dA_C}{d\ln N_d} = \frac{A_C(1-A_C)}{3}\left(1 + \frac{5}{2}\frac{d\ln LWP}{d\ln N_d}\right) \quad (6)$$

where S is the sensitivity of cloud albedo to N_d. A_c is calculated from τ based on a general expression for two-stream approximation solution (Glenn et al., 2020):

$$A_c = \frac{\tau}{13.33 + \tau} \quad (7)$$

The first term of Eq. (6) refers to the changes in albedo due to the changes in N_d, while holding the LWP (i.e. Twomey effect). The second term, which accounts for LWP adjustment, can regulate the Twomey effect. The Twomey effect is completely offset when $\frac{d\ln LWP}{d\ln N_d}$ equals –2/5. Figure 7 shows the diurnal variations of S, calculated with Eq. (6) using the diurnal variations of both A_c and LWP

adjustments. To isolate their individual influence, S was calculated using MODIS-averaged value for either A_c or LWP adjustments while retaining the diurnal variation for the other (Fig. S18). Given the minimal diurnal fluctuation in $\frac{A_C(1-A_C)}{3}$, the diurnal variations of S are mainly controlled by LWP adjustments. According to Fig. 7, if S is evaluated only at fixed moments (e.g. the average value during MODIS overpasses for Terra at 1030 LT and Aqua at 1330 LT), the cooling effect of S is consistently underestimated before 1100 LT, with a maximum bias of 89% at 0800 LT. At 1300 LT, S even turns negative, suggesting that albedo decreases with increasing N_d, which has been reported in previous studies (Zhang et al., 2022). The negative S is possibly linked to strong decoupling over the AUW region at 1300 LT as discussed in Section 3.2. In the ECS region, the associated bias spans from a 24% overestimation at 0800 LT to a 40% underestimation at 1600 LT. The results highlight the critical need to account for diurnal variations of LWP adjustments when assessing the aerosol indirect effect. Future studies should incorporate geostationary observations or high-resolution simulations to better constrain the diurnal effects of LWP adjustments.

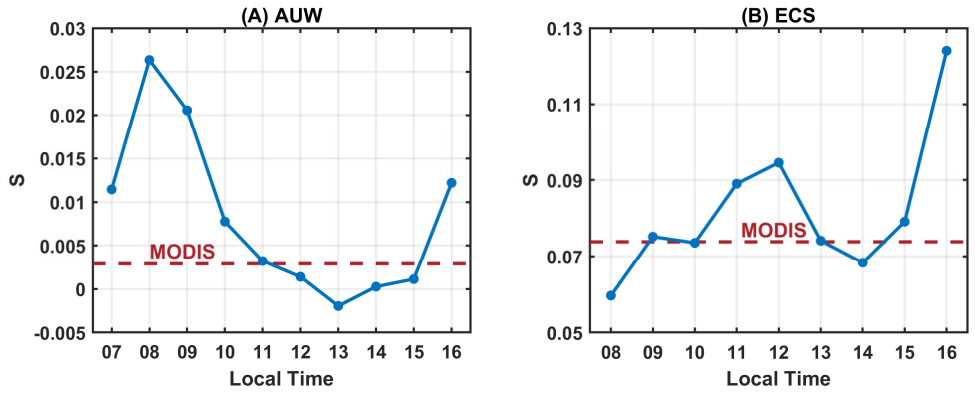

Figure 7. The diurnal variations of S calculated by Eq. (6) in the (A) AUW and (B) ECS (blue lines). The red dashed lines represent the average values during MODIS Terra (1030 LT) and Aqua (1330 LT) overpasses.".

22. Discussion section: The criticism of Qiu et al. (2024) does not make sense. I would argue that the methodology in Qiu et al. was more carefully crafted than the one in Li et al. 2025.Also the stratification by cloud thickness is flawed because both LWP and thickness are a function of optical depth, so both parameters are NOT independent.

Response: Thank you for your comments! As suggested by the previous reviewer, we added a comparison rather than criticism with Qiu et al. (2024) in the discussion section about similarities and differences in our conclusions. Both studies recognize that changes in cloud thickness drive the diurnal variations of LWP adjustments, yet the underlying physical interpretations are entirely different.

Qiu et al. (2024) calculated LWP adjustments within 1°×1° grid, which offers the advantage of

assuming negligible meteorological influence. In contrast, our approach calculates LWP adjustments using all 1° scenes. Furthermore, Qiu et al. (2024) focused on the evolution of cloud thickness at fixed grids, whereas in our study, thickness serves as an indicator to isolate meteorological covariations following Rosenfeld et al., (2019). Thus, we emphasize how varying meteorological and dynamical conditions at different times drive LWP adjustments.

We have rephrased the discussion about Qiu et al. (2024) to be clearer (see Lines 491-498): "Our observed diurnal LWP adjustment pattern in the AUW region is consistent with Qiu et al. (2024)'s findings in the eastern North Atlantic, where thick-thin cloud transitions dominated daytime variability. However, the main drivers emphasized in the two studies are different. Qiu et al. (2024) calculated LWP adjustment within each 1° grid box to minimize the meteorological covariations and highlighted cloud-intrinsic evolution, whereas we retain these covariations and then disentangle their influence by cloud thickness stratification analyses following Rosenfeld et al. (2019). Consequently, we attribute the diurnal variations in LWP adjustments mainly to temporal changes in meteorological and dynamical conditions. Additionally, after 1300 LT, cloud thickness remains relatively stable; the weakening of negative LWP adjustments is linked to reduced entrainment as large-scale subsidence strengthens (Fig. 4A).

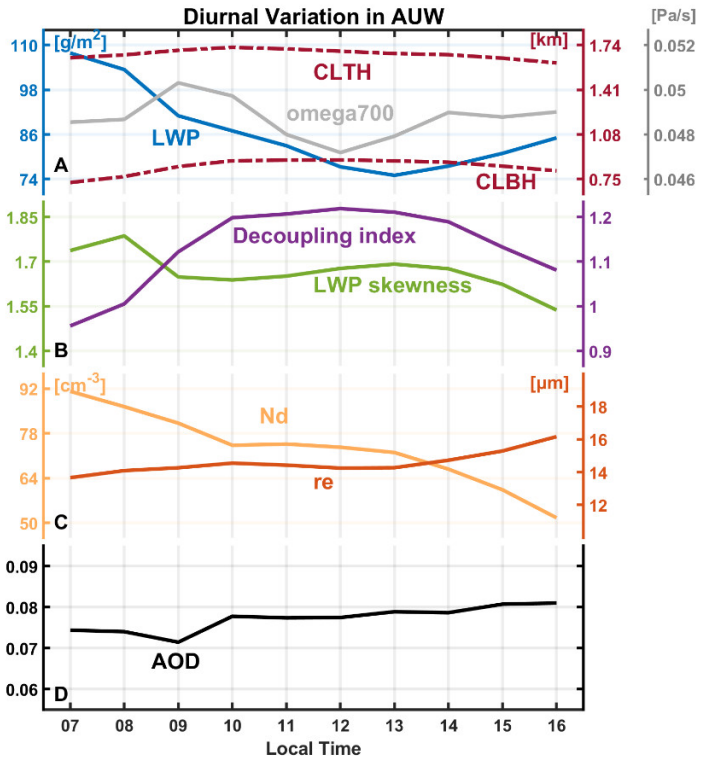

Figure 4. Diurnal patterns in the AUW region. (A) Cloud liquid water path (LWP), cloud-top height (CLTH), cloud base height (CLBH), and vertical velocity on 700 hPa (omega700, positive values indicate downdraft) from ERA5 reanalysis. (B) LWP skewness and decoupling index in the AUW region. (C) Cloud droplet number concentration (N_d) and effective radius (r_e). (D) Aerosol optical depth (AOD)."

We agree that LWP and cloud thickness are not independent, but the stratification by cloud thickness remains physically meaningful. Cloud thickness typically serves as a mediator for large-scale meteorology (such as cold air advection, boundary layer decoupling, and surface heat fluxes) to influence LWP. These processes are particularly evident in the ECS region, where the increase in LWP at high N_d corresponds with an increase in cloud thickness (Fig. R4B). Additionally, cloud thickness alters LWP by influencing cloud microphysical processes, such as promoting condensation growth. Fons et al. (2023) suggested cloud thickness is an important confounder in the N_d-LWP relationship that should be conditioned on. Constraining cloud thickness effectively limits the vertical development of clouds, which restricts the changes in LWP driven by vertical cloud evolution, thereby suppressing thickness-driven variability.

Once H is fixed within a narrow bin, the range of allowable LWP driven solely by vertical growth is capped. What remains is LWP variability arising from microphysics (droplet size, number), exactly the signal we want to isolate. Therefore, the stratification of cloud thickness can isolate a significant portion of covariations, highlighting the impact of N_d on LWP. According to Rosenfeld et al. (2019), for a given cloud thickness, N_d accounts for nearly half of the observed LWP variations. Therefore, although LWP, H, and optical depth are algebraically related, fixing H effectively decouples the dynamic envelope from the microphysics, making the N_d-LWP relationship conditionally independent and scientifically meaningful.

We have added discussions of using H for interpreting the N_d-LWP relationship (see Lines 261-293): "The above results suggest that the impact of large-scale meteorology on cloud microphysical processes ultimately determines the pattern of LWP adjustment. Previous studies employed various methods to exclude environmental confounding factors, such as opportunistic experiments from ship-track or volcano eruptions (Chen et al., 2022; Toll et al., 2019), where an overall weak LWP adjustment was observed. For satellite studies, Rosenfeld et al. (2019) pointed out that cloud thickness (H) constrained most of the meteorological impacts, and N_d explained nearly half of the LWP variability for a given H. They demonstrated an overall positive LWP adjustment when separating H. However, we find that LWP adjustments become negative after constraining H in the intervals of Fig. 3 (B and E), indicating the dominant effect of entrainment-feedbacks. The discrepancy may arise from their focus on samples in convective cores (top 10% of cloud optical thickness), which are closer to adiabatic, whereas our samples suggest more exchange with the free atmosphere.

Here, our results indicate the physical significance of constraining H. In the AUW region, negative LWP adjustments become weaker as H increases (Fig. 3B). H alters LWP adjustments by influencing cloud microphysical processes, such as promoting condensation growth (Fons et al.,

2023). Thicker clouds with higher cloud-top r_e are less sensitive to entrainment-feedbacks with increasing N_d compared to thinner clouds. In other words, LWP in different H intervals responds differently to N_d, so it is necessary to restrict H to exclude the effects of covariations. However, in the ECS region, negative LWP adjustments for clouds with H < 900 m become stronger with increasing H, while for clouds with H > 900 m, quite the contrary: it weakens with increasing H (Fig. 3E). The bidirectional sensitivity of LWP adjustments to H is likely attributed to distinct mixing characteristics among different cloud regimes in the ECS region. Constraining H in the ECS region restricts a majority of mechanisms influencing cloud vertical development. Cloud thickness typically serves as a mediator for large-scale meteorology (such as cold air advection, LTS, and surface heat fluxes) to influence LWP. These processes are particularly evident in the ECS region, where the increase in LWP at high N_d corresponds with an increase in cloud thickness (Fig. 2B). Therefore, the stratification of cloud thickness can isolate a significant portion of covariations, highlighting the impact of N_d on LWP.

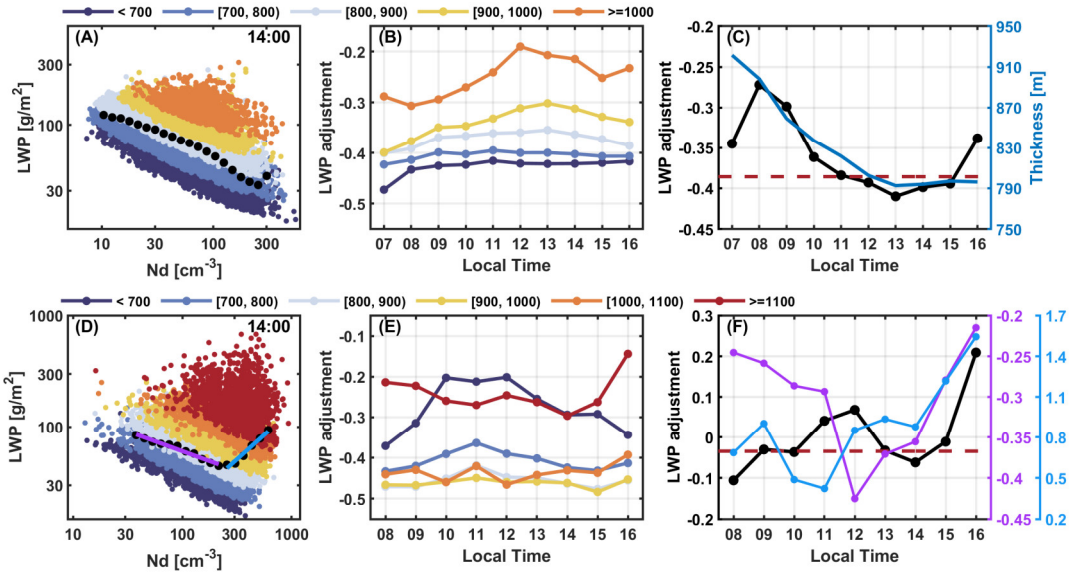

Figure 3. LWP adjustments in log-log spaces and their diurnal patterns in two typical regions (the west of Australia, AUW and the East China Sea, ECS). Cloud samples are scattered in N_d-LWP log space at 1400 LT in the (A) AUW and (D) ECS region. The complete pictures of all available daytime are presented in Fig. S11. Colored dots are samples in different cloud thickness (H) bins (unit: m). Black dots represent the median LWP in each N_d bin. The colored lines are the fits of black dots at different stages in the ECS region. Diurnal variations of LWP adjustments binned by H in the (B) AUW and (E) ECS regions are shown. Colored lines in (F) are diurnal variations of different stages in (D), while black lines in (C) and (F) are the overall diurnal variations of LWP adjustments in two regions, respectively. The blue line in (C) represents the diurnal variation of H. Red dashed lines represent the average LWP adjustments during MODIS Terra (1030 LT) and Aqua (1330 LT) overpasses, –0.39 for the AUW region (C) and –0.03 for the ECS region (F).".

23. What is the physical process that would explain the convective invigoration? Why is this the only plausible explanation. For example, postfrontal conditions and cold-air outbreaks could explain both an increase in both LWP and Nd. In my opinion, the convective invigoration explanation is not proved by the analysis. The use of LTS is not optimal because LTS explains a modest fraction of cloud variance, so not finding a relationship between cloud microphysics and LTS does not mean much.

Response: We highly appreciate these constructive comments raised by the reviewer. We agree that attributing the positive LWP adjustments at high N_d solely to warm invigoration is insufficient. As described above in response to Comment 18, our revised analysis confirms that large-scale meteorology, especially the cold air advection, is the main driver of the observed LWP increase at high N_d (> ~300 cm^{-3}) in the ECS region. This is supported by the significant meteorological transitions across the turning point of the V shape (Fig. R4). The aerosol-rich, relatively cold and dry air from continent reduces the stability of the sub-cloud layer, triggering the release of water vapor into the boundary layer and subsequently promoting cloud droplet activation and development of thicker clouds. Additionally, we agree that LTS explains only a modest fraction of cloud variance, while the increase in LWP at high N_d results from the combined influence of meteorological conditions. Thus, we incorporated additional variables in Fig. R4 to disentangle the impact of meteorological factors on cloud microphysical processes.

We acknowledge cold air outbreaks (CAOs) could explain the increase in both N_d and LWP, but CAOs are more likely to be a strong form of cold air advection. Our analysis reveals the seasonal dependence of CAOs. Following Papritz et al. (2015), the CAO Index (CAOI) was calculated as the difference in potential temperature between the surface skin and 850 hPa. CAO events are identified when the CAO Index is greater than zero. CAOs are most pronounced in autumn and winter, with no significant occurrence in spring (Fig. R6). Results of summer are statistically insignificant due to the limited samples (3%), especially after eliminating the samples with strong precipitation by applying the threshold (GPM = 0 mm hr^{-1}). The seasonal variations are consistent with the East Asian monsoon, where strong northerly winds prevail in winter but weaken in spring (Liu et al., 2016), leading to reduced CAOI. However, the impacts of cold air advection are prevalent throughout the seasons (Fig. R7), making it a more plausible reason for the observed sub-cloud destabilization and subsequent increases in N_d and LWP.

We have added the discussion of CAOs in the revised manuscript (see Lines 244-253): "While cold air outbreaks (CAOs) also contribute to the observed increases in both N_d and LWP, our analysis suggests that cold air advection is a more consistent and seasonally pervasive driver and CAOs represent a strong form of cold air advection. Following Papritz et al. (2015), the Cold Air Outbreak

Index (CAOI) was calculated as the difference in potential temperature between the surface skin and 850 hPa. CAO events are identified when CAOI > 0. Our results indicate that CAOs are most pronounced in autumn and winter, with no significant occurrence in spring (Fig. S5). Results of summer are statistically insignificant due to the limited samples (3%), particularly after excluding cases with strong precipitation (GPM = 0 mm hr^{-1}). The seasonal variations are consistent with the East Asian monsoon, where strong northerly winds prevail in winter but weaken in spring (Liu et al., 2016), leading to reduced CAOI. In contrast, the impacts of cold air advection are prevalent throughout the seasons (Fig. S6), making it a more plausible reason for the observed sub-cloud destabilization and subsequent increases in N_d and LWP.".

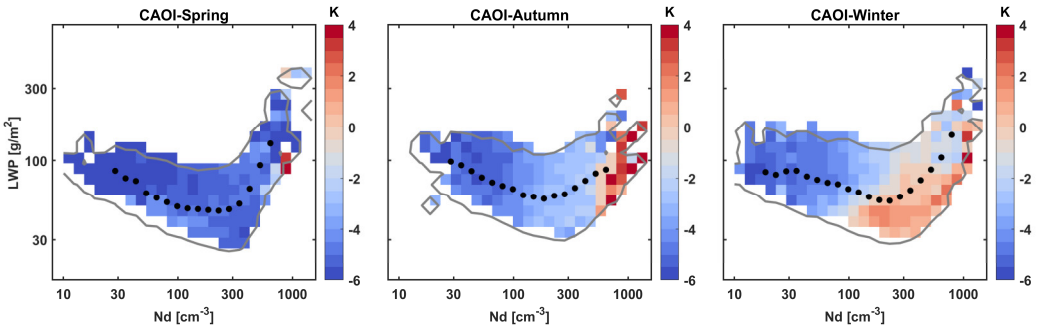

Figure R6. The median cold-air outbreak index (CAOI) in N_d-LWP log-log space for spring, autumn, and winter in the ECS region. Among the total samples (173181), spring, summer, autumn, and winter account for 31%, 3%, 22%, and 44%, respectively. Due to the limited samples (3%), results of summer are statistical insignificance, especially after eliminating the samples with strong precipitation by applying the threshold (GPM = 0 mm hr^{-1}). **The figures are the same as Figure S5 in the revised manuscript.**

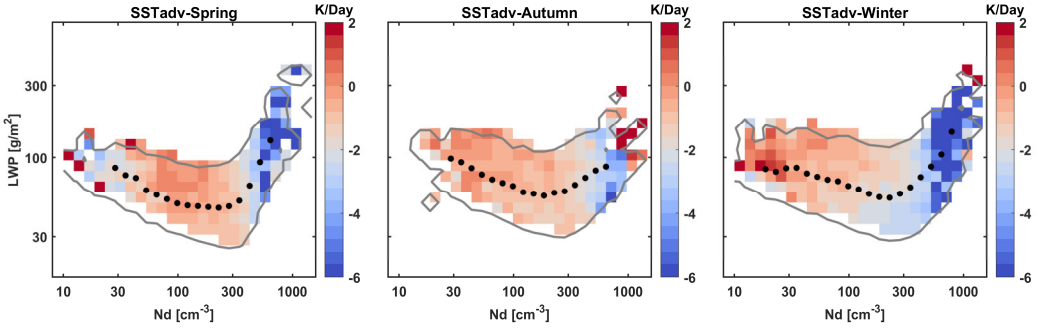

Figure R7. The median horizontal temperature advection at the surface (SST_{adv}) in N_d-LWP log-log space for spring, autumn, and winter in the ECS region. The figures are the same as Figure S6 in the revised manuscript.

Reference

Albrecht, B. A.: Aerosols, Cloud Microphysics, and Fractional Cloudiness, Science, 245, 1227–1230, https://doi.org/10.1126/science.245.4923.1227, 1989.

Albrecht, B. A., Bretherton, C. S., Johnson, D., Scubert, W. H., and Frisch, A. S.: The Atlantic Stratocumulus Transition Experiment—ASTEX, Bulletin of the American Meteorological Society, 76, 889–904, https://doi.org/10.1175/1520-0477(1995)076<0889:TASTE>2.0.CO;2, 1995.

Bellouin, N., Quaas, J., Gryspeerdt, E., Kinne, S., Stier, P., Watson-Parris, D., Boucher, O., Carslaw, K. S., Christensen, M., Daniau, A. -L., Dufresne, J. -L., Feingold, G., Fiedler, S., Forster, P., Gettelman, A., Haywood, J. M., Lohmann, U., Malavelle, F., Mauritsen, T., McCoy, D. T., Myhre, G., Mülmenstädt, J., Neubauer, D., Possner, A., Rugenstein, M., Sato, Y., Schulz, M., Schwartz, S. E., Sourdeval, O., Storelvmo, T., Toll, V., Winker, D., and Stevens, B.: Bounding Global Aerosol Radiative Forcing of Climate Change, Rev. Geophys., 58, https://doi.org/10.1029/2019RG000660, 2020.

Bender, F. A.-M., Frey, L., McCoy, D. T., Grosvenor, D. P., and Mohrmann, J. K.: Assessment of aerosol–cloud–radiation correlations in satellite observations, climate models and reanalysis, Clim Dyn, 52, 4371–4392, https://doi.org/10.1007/s00382-018-4384-z, 2019.

Brenguier, J.-L., Burnet, F., and Geoffroy, O.: Cloud optical thickness and liquid water path – does the *k* coefficient vary with droplet concentration?, Atmospheric Chemistry and Physics, 11, 9771–9786, https://doi.org/10.5194/acp-11-9771-2011, 2011.

Cao, Y., Zhu, Y., Wang, M., Rosenfeld, D., Liang, Y., Liu, J., Liu, Z., and Bai, H.: Emission Reductions Significantly Reduce the Hemispheric Contrast in Cloud Droplet Number Concentration in Recent Two Decades, Journal of Geophysical Research: Atmospheres, 128, e2022JD037417, https://doi.org/10.1029/2022JD037417, 2023.

Chen, Y., Haywood, J., Wang, Y., Malavelle, F., Jordan, G., Partridge, D., Fieldsend, J., De Leeuw, J., Schmidt, A., Cho, N., Oreopoulos, L., Platnick, S., Grosvenor, D., Field, P., and Lohmann, U.: Machine learning reveals climate forcing from aerosols is dominated by increased cloud cover, Nat. Geosci., 15, 609–614, https://doi.org/10.1038/s41561-022-00991-6, 2022.

Drueke, S., Kirshbaum, D. J., and Kollias, P.: Environmental sensitivities of shallow-cumulus dilution – Part 1: Selected thermodynamic conditions, Atmospheric Chemistry and Physics, 20, 13217–13239, https://doi.org/10.5194/acp-20-13217-2020, 2020.

Feingold, G., Glassmeier, F., Zhang, J., and Hoffmann, F.: Opinion: Inferring Process from Snapshots of Cloud Systems, EGUsphere, 1–28, https://doi.org/10.5194/egusphere-2025-1869, 2025.

Fons, E., Runge, J., Neubauer, D., and Lohmann, U.: Stratocumulus adjustments to aerosol perturbations disentangled with a causal approach, npj Clim Atmos Sci, 6, 130, https://doi.org/10.1038/s41612-023-00452-w, 2023.

Glassmeier, F., Hoffmann, F., Johnson, J. S., Yamaguchi, T., Carslaw, K. S., and Feingold, G.: Aerosol-cloud-climate cooling overestimated by ship-track data, Science, 371, 485–489, https://doi.org/10.1126/science.abd3980, 2021.

Glenn, I. B., Feingold, G., Gristey, J. J., and Yamaguchi, T.: Quantification of the Radiative Effect of Aerosol–Cloud Interactions in Shallow Continental Cumulus Clouds, https://doi.org/10.1175/JAS-D-19-0269.1, 2020.

Goren, T., Choudhury, G., Kretzschmar, J., and McCoy, I.: Co-variability drives the inverted-V sensitivity between liquid water path and droplet concentrations, Atmospheric Chemistry and Physics, 25, 3413–3423, https://doi.org/10.5194/acp-25-3413-2025, 2025.

Grosvenor, D. P., Sourdeval, O., Zuidema, P., Ackerman, A., Alexandrov, M. D., Bennartz, R., Boers, R., Cairns, B., Chiu, J. C., Christensen, M., Deneke, H., Diamond, M., Feingold, G., Fridlind, A., Hünerbein, A., Knist, C., Kollias, P., Marshak, A., McCoy, D., Merk, D., Painemal, D., Rausch, J., Rosenfeld, D., Russchenberg, H., Seifert, P., Sinclair, K., Stier, P., van Diedenhoven, B., Wendisch, M., Werner, F., Wood, R., Zhang, Z., and Quaas, J.: Remote Sensing of Droplet Number Concentration in Warm Clouds: A Review of the Current State of Knowledge and Perspectives, Reviews of Geophysics, 56, 409–453, https://doi.org/10.1029/2017RG000593, 2018.

Gryspeerdt, E., Goren, T., Sourdeval, O., Quaas, J., Mülmenstädt, J., Dipu, S., Unglaub, C., Gettelman, A., and Christensen, M.: Constraining the aerosol influence on cloud liquid water path, Atmos. Chem. Phys., 19, 5331–5347, https://doi.org/10.5194/acp-19-5331-2019, 2019.

Gryspeerdt, E., Povey, A. C., Grainger, R. G., Hasekamp, O., Hsu, N. C., Mulcahy, J. P., Sayer, A. M., and Sorooshian, A.: Uncertainty in aerosol–cloud radiative forcing is driven by clean conditions, Atmos. Chem. Phys., 23, 4115–4122, https://doi.org/10.5194/acp-23-4115-2023, 2023.

Heus, T., Dijk, G. van, Jonker, H. J. J., and Akker, H. E. A. V. den: Mixing in Shallow Cumulus Clouds Studied by Lagrangian Particle Tracking, https://doi.org/10.1175/2008JAS2572.1, 2008.

Huffman, G. J., Bolvin, D. T., Braithwaite, D., Hsu, K.-L., Joyce, R. J., Kidd, C., Nelkin, E. J., Sorooshian, S., Stocker, E. F., Tan, J., Wolff, D. B., and Xie, P.: Integrated Multi-satellite Retrievals for the Global Precipitation Measurement (GPM) Mission (IMERG), in: Satellite Precipitation Measurement: Volume 1, edited by: Levizzani, V., Kidd, C., Kirschbaum, D. B., Kummerow, C. D., Nakamura, K., and Turk, F. J., Springer International Publishing, Cham, 343–353, https://doi.org/10.1007/978-3-030-24568-9_19, 2020.

Klein, S. A. and Hartmann, D. L.: The Seasonal Cycle of Low Stratiform Clouds, Journal of Climate, 6, 1587–1606, https://doi.org/10.1175/1520-0442(1993)006<1587:TSCOLS>2.0.CO;2, 1993.

Liu, J.-W., Xie, S.-P., Yang, S., and Zhang, S.-P.: Low-Cloud Transitions across the Kuroshio Front in the East China Sea, Journal of Climate, 29, 4429–4443, https://doi.org/10.1175/JCLI-D-15-0589.1, 2016.

Long, J., Wang, Y., Zhang, S., and Liu, J.: Transition of Low Clouds in the East China Sea and Kuroshio Region in Winter: A Regional Atmospheric Model Study, Journal of Geophysical Research: Atmospheres, 125, e2020JD032509, https://doi.org/10.1029/2020JD032509, 2020.

Martin, G. M., Johnson, D. W., and Spice, A.: The Measurement and Parameterization of Effective Radius of Droplets in Warm Stratocumulus Clouds, Journal of the Atmospheric Sciences, 51, 1823–1842, https://doi.org/10.1175/1520-0469(1994)051<1823:TMAPOE>2.0.CO;2, 1994.

Mellado, J. P.: Cloud-Top Entrainment in Stratocumulus Clouds, Annu. Rev. Fluid Mech., 49, 145–169, https://doi.org/10.1146/annurev-fluid-010816-060231, 2017.

Michibata, T., Suzuki, K., Sato, Y., and Takemura, T.: The source of discrepancies in aerosol–cloud–precipitation interactions between GCM and A-Train retrievals, Atmos. Chem. Phys., 16, 15413–15424, https://doi.org/10.5194/acp-16-15413-2016, 2016.

Minnis, P., Sun-Mack, S., Young, D. F., Heck, P. W., Garber, D. P., Chen, Y., Spangenberg, D. A., Arduini, R. F., Trepte, Q. Z., Smith, W. L., Ayers, J. K., Gibson, S. C., Miller, W. F., Hong, G., Chakrapani, V., Takano, Y., Liou, K.-N., Xie, Y., and Yang, P.: CERES Edition-2 Cloud Property Retrievals Using TRMM VIRS and Terra and Aqua MODIS Data—Part I: Algorithms, IEEE Trans. Geosci. Remote Sensing, 49, 4374–4400, https://doi.org/10.1109/TGRS.2011.2144601, 2011.

Minnis, P., Sun-Mack, S., Chen, Y., Chang, F.-L., Yost, C. R., Smith, W. L., Heck, P. W., Arduini, R. F., Bedka, S. T., Yi, Y., Hong, G., Jin, Z., Painemal, D., Palikonda, R., Scarino, B. R., Spangenberg, D. A., Smith, R. A., Trepte, Q. Z., Yang, P., and Xie, Y.: CERES MODIS Cloud Product Retrievals for Edition 4—Part I: Algorithm Changes, IEEE Transactions on Geoscience and Remote Sensing, 59, 2744–2780, https://doi.org/10.1109/TGRS.2020.3008866, 2021.

Painemal, D. and Zuidema, P.: Assessment of MODIS cloud effective radius and optical thickness retrievals over the Southeast Pacific with VOCALS-REx in situ measurements, Journal of Geophysical Research: Atmospheres, 116, https://doi.org/10.1029/2011JD016155, 2011.

Papritz, L., Pfahl, S., Sodemann, H., and Wernli, H.: A Climatology of Cold Air Outbreaks and Their Impact on Air–Sea Heat Fluxes in the High-Latitude South Pacific, https://doi.org/10.1175/JCLI-D-14-00482.1, 2015.

Qiu, S., Zheng, X., Painemal, D., Terai, C. R., and Zhou, X.: Daytime variation in the aerosol indirect effect for warm marine boundary layer clouds in the eastern North Atlantic, Atmospheric Chemistry and Physics, 24, 2913–2935, https://doi.org/10.5194/acp-24-2913-2024, 2024.

Rosenfeld, D., Wang, H., and Rasch, P. J.: The roles of cloud drop effective radius and LWP in determining rain properties in marine stratocumulus, Geophysical Research Letters, 39, https://doi.org/10.1029/2012GL052028, 2012.

Rosenfeld, D., Zhu, Y., Wang, M., Zheng, Y., Goren, T., and Yu, S.: Aerosol-driven droplet concentrations dominate coverage and water of oceanic low-level clouds, Science, 363, eaav0566, https://doi.org/10.1126/science.aav0566, 2019.

Scott, R. C., Myers, T. A., Norris, J. R., Zelinka, M. D., Klein, S. A., Sun, M., and Doelling, D. R.: Observed Sensitivity of Low-Cloud Radiative Effects to Meteorological Perturbations over the Global Oceans, Journal of Climate, 33, 7717–7734, https://doi.org/10.1175/JCLI-D-19-1028.1, 2020.

Small, J. D., Chuang, P. Y., and Jonsson, H. H.: Microphysical imprint of entrainment in warm cumulus, Tellus B: Chemical and Physical Meteorology, 65, https://doi.org/10.3402/tellusb.v65i0.19922, 2013.

Smalley, K. M., Lebsock, M. D., and Eastman, R.: Diurnal Patterns in the Observed Cloud Liquid Water Path Response to Droplet Number Perturbations, Geophysical Research Letters, 51, e2023GL107323, https://doi.org/10.1029/2023GL107323, 2024.

Stevens, B., Lenschow, D. H., Vali, G., Gerber, H., Bandy, A., Blomquist, B., Brenguier, J.-L., Bretherton, C. S., Burnet, F., Campos, T., Chai, S., Faloona, I., Friesen, D., Haimov, S., Laursen, K., Lilly, D. K., Loehrer, S. M., Malinowski, S. P., Morley, B., Petters, M. D., Rogers, D. C., Russell, L., Savic-Jovcic, V., Snider, J. R., Straub, D., Szumowski, M. J., Takagi, H., Thornton, D. C., Tschudi, M., Twohy, C., Wetzel, M., and Zanten, M. C. van: Dynamics and Chemistry of Marine Stratocumulus—DYCOMS-II, https://doi.org/10.1175/BAMS-84-5-579, 2003.

Sun-Mack, S., Minnis, P., Chen, Y., Kato, S., Yi, Y., Gibson, S. C., Heck, P. W., and Winker, D. M.: Regional Apparent Boundary Layer Lapse Rates Determined from CALIPSO and MODIS Data for Cloud-Height Determination, https://doi.org/10.1175/JAMC-D-13-081.1, 2014.

Toll, V., Christensen, M., Quaas, J., and Bellouin, N.: Weak average liquid-cloud-water response to anthropogenic aerosols, Nature, 572, 51–55, https://doi.org/10.1038/s41586-019-1423-9, 2019.

Towers, S.: Potential fitting biases resulting from grouping data into variable width bins, Physics Letters B, 735, 146–148, https://doi.org/10.1016/j.physletb.2014.06.023, 2014.

Twomey, S.: The Influence of Pollution on the Shortwave Albedo of Clouds, Journal of the Atmospheric Sciences, 34, 1149–1152, https://doi.org/10.1175/1520-0469(1977)034<1149:TIOPOT>2.0.CO;2, 1977.

Wang, Y., Zhao, C., McFarquhar, G. M., Wu, W., Reeves, M., and Li, J.: Dispersion of Droplet Size Distributions in Supercooled Non-precipitating Stratocumulus from Aircraft Observations Obtained during the Southern Ocean Cloud Radiation Aerosol Transport Experimental Study, Journal of Geophysical Research: Atmospheres, 126, e2020JD033720, https://doi.org/10.1029/2020JD033720, 2021.

Wood, R.: Drizzle in Stratiform Boundary Layer Clouds. Part I: Vertical and Horizontal Structure, https://doi.org/10.1175/JAS3529.1, 2005.

Wood, R., Mechoso, C. R., Bretherton, C. S., Weller, R. A., Huebert, B., Straneo, F., Albrecht, B. A., Coe, H., Allen, G., Vaughan, G., Daum, P., Fairall, C., Chand, D., Gallardo Klenner, L., Garreaud, R., Grados, C., Covert, D. S., Bates, T. S., Krejci, R., Russell, L. M., de Szoeke, S., Brewer, A., Yuter, S. E., Springston, S. R., Chaigneau, A., Toniazzo, T., Minnis, P., Palikonda, R., Abel, S. J., Brown, W. O. J., Williams, S., Fochesatto, J., Brioude, J., and Bower, K. N.: The VAMOS Ocean-Cloud-Atmosphere-Land Study Regional Experiment (VOCALS-REx): goals, platforms, and field operations, Atmospheric Chemistry and Physics, 11, 627–654, https://doi.org/10.5194/acp-11-627-2011, 2011.

Zhang, J., Zhou, X., Goren, T., and Feingold, G.: Albedo susceptibility of northeastern Pacific stratocumulus: the role of covarying meteorological conditions, Atmospheric Chemistry and Physics, 22, 861–880, https://doi.org/10.5194/acp-22-861-2022, 2022.

Zhang, X., Wang, H., Che, H.-Z., Tan, S.-C., Yao, X.-P., Peng, Y., and Shi, G.-Y.: Radiative forcing of the aerosol-cloud interaction in seriously polluted East China and East China Sea, Atmospheric Research, 252, 105405, https://doi.org/10.1016/j.atmosres.2020.105405, 2021.

Zhou, X. and Feingold, G.: Impacts of Mesoscale Cloud Organization on Aerosol-Induced Cloud Water Adjustment and Cloud Brightness, Geophysical Research Letters, 50, e2023GL103417, https://doi.org/10.1029/2023GL103417, 2023.